

Interaction mechanism between the focused ultrasound and lipid membrane at the molecular level

Cite as: J. Chem. Phys. **150**, 215101 (2019); <https://doi.org/10.1063/1.5099008>

Submitted: 05 April 2019 . Accepted: 13 May 2019 . Published Online: 03 June 2019

Viet Hoang Man , Mai Suan Li , Junmei Wang, Philippe Derreumaux, and Phuong H. Nguyen 



[View Online](#)



[Export Citation](#)



[CrossMark](#)

ARTICLES YOU MAY BE INTERESTED IN

[A novel approach to describe chemical environments in high-dimensional neural network potentials](#)

The Journal of Chemical Physics **150**, 154102 (2019); <https://doi.org/10.1063/1.5086167>

[Molecular polarizability in open ensemble simulations of aqueous nanoconfinements under electric field](#)

The Journal of Chemical Physics **150**, 164702 (2019); <https://doi.org/10.1063/1.5094170>

[Neural network based quasi-diabatic Hamiltonians with symmetry adaptation and a correct description of conical intersections](#)

The Journal of Chemical Physics **150**, 214101 (2019); <https://doi.org/10.1063/1.5099106>

Lock-in Amplifiers up to 600 MHz

starting at

\$6,210



 Zurich
Instruments

[Watch the Video](#) 

Interaction mechanism between the focused ultrasound and lipid membrane at the molecular level

Cite as: J. Chem. Phys. 150, 215101 (2019); doi: 10.1063/1.5099008

Submitted: 5 April 2019 • Accepted: 13 May 2019 •

Published Online: 3 June 2019



View Online



Export Citation



CrossMark

Viet Hoang Man,¹ Mai Suan Li,^{2,3} Junmei Wang,¹ Philippe Derreumaux,⁴ and Phuong H. Nguyen^{4,a}

AFFILIATIONS

¹ Department of Pharmaceutical Sciences, School of Pharmacy, University of Pittsburgh, Pittsburgh, Pennsylvania 15213, USA

² Institute of Physics, Polish Academy of Sciences, Al. Lotników 32/46, 02-668 Warsaw, Poland

³ Institute for Computational Science and Technology, SBI Building, Quang Trung Software City, Tan Chanh Hiep Ward, District 12, Ho Chi Minh City, Vietnam

⁴ Laboratoire de Biochimie Théorique UPR 9080, CNRS, Université Denis Diderot, Sorbonne Paris Cité IBPC, 13 rue Pierre et Marie Curie, 75005 Paris, France

^a Author to whom correspondence should be addressed: nguyen@ibpc.fr

ABSTRACT

Focused ultrasound (FUS) has a wide range of medical applications. Nowadays, the diagnostic and therapeutic ultrasound procedures are routinely used; effects of ultrasound on biological systems at the molecular level are, however, not fully understood. Experimental results on the interaction of the cell membrane, a simplest but important system component, with ultrasound are controversial. Molecular dynamics (MD) simulations could provide valuable insights, but there is no single study on the mechanism of the FUS induced structural changes in cell membranes. With this in mind, we develop a simple method to include FUS into a standard MD simulation. Adopting the 1,2-dioleoyl-sn-glycero-3-phosphocholine lipid membrane as a representative model described by the MARTINI coarse-grained force field, and using experimental values of the ultrasound frequency and intensity, we show that the heat and bubble cavitation are not the primary direct mechanisms that cause structural changes in the membrane. The spatial pressure gradients between the focused and free regions and between the parallel and perpendicular directions to the membrane are the origin of the mechanism. These gradients force lipids to move out of the focused region, forming a lipid flow along the membrane diagonal. Lipids in the free region move in the opposite direction due to the conservation of the total momentum. These opposite motions create wrinkles along the membrane diagonal at low FUS intensities and tear up the membrane at high FUS intensities. Once the membrane is torn up, it is not easy to reform. The implication of our findings in the FUS-induced drug delivery is discussed in some detail.

Published under license by AIP Publishing. <https://doi.org/10.1063/1.5099008>

I. INTRODUCTION

Ultrasound has a wide range of medical applications. A major development and application of ultrasound methods and devices for clinical diagnostics, surgery, and therapy started in the 1950s, and exponentially expanded during the last few decades.¹ In parallel, numerous studies have been carried out to address possible side effects of therapeutic ultrasound, including bioeffects, hazards, and safety.² Important applications are the use of high intensity focused ultrasound (FUS) in treatments of prostate cancer, essential tremors, and pain from bone metastasis,³ and low intensity FUS in

the opening of the blood-brain-barrier (BBB) for drug delivery.^{4,5} The use of FUS allows one to concentrate the ultrasound power to a specific region, avoiding the damage of surrounding regions. It has been suggested that the main mechanisms of high intensity FUS and tissue interaction involve thermal and mechanical effects. The high intensity FUS could elevate local tissue temperature to higher than 60 °C by the thermal effect, causing tumor cell destruction. The mechanical effects include microstreaming, cavitation, and radiation force. Under ultrasound, tiny gas bubbles may be formed in the tissue or solution. The stable cavitation occurs when bubbles oscillate stably in size, creating shear stress, microstreaming on the

surrounding objects.^{6–10} The collapse of bubbles, called inertial cavitation, results in a high temperature and shock wave that disintegrate the surrounding tissues.^{11–15} The ultrasound radiation force caused by spatial gradients in acoustic intensity could induce tissue displacement.¹ The low intensity FUS is usually combined with injected gas filled microbubbles.⁴ When the bubbles reach the ultrasound field, they vibrate and exert mechanical force on the BBB. It has been suggested that the BBB is opened due to the disruption of the tight junctions connecting neighboring endothelial cells of the BBB. This allows therapeutic molecules to move from the blood to the brain.¹⁶ Although all these applications are promising, effects of high and low intensity FUS on biological systems are not fully understood at the molecular level, even for simplest system components such as cell membranes. Some important questions, which provide a motivation for this work, are whether the low intensity FUS induces BBB opening at the tight junctions as believed or tears up the cell membrane, allowing cells to uptake drugs bound to their surface? Whether the bubble cavitation or ultrasound radiation force in high intensity FUS experiments is the main effect on the membrane? Answering these questions at the molecular level is probably very difficult for experiments. Indeed, experimental results on the synthetic lipid bilayers are controversial. Some studies have shown that lipid bilayers do not respond to low intensity ultrasound,^{17–19} but a recent experiment has shown that ultrasound radiation force causes oscillation and displacement of lipid membranes, resulting in small changes in membrane area and capacitance.²⁰

From the theoretical side, a number of simulations have been carried out to study the bubble inertial cavitation and the effect of the shock wave on the lipid bilayer structure, employing continuum,²¹ coarse-grained, and atomistic molecular models.^{22–30} Recently, we have developed a bubble model for molecular dynamics (MD) simulations of the stable cavitation.³¹ The model has been applied to study the effects of stable cavitation on the amyloid fibril and lipid membrane models,^{31,32} and to verify the Rayleigh-Plesset equation for the description of the dynamics of nanosized bubbles.³³ However, we have not seen in the literature any MD simulations aimed at studying the direct interaction between FUS and the membrane. To this end, the core aim of this work is two folds: (i) develop a nonequilibrium MD (NEMD) simulation method that extends well-established MD simulation techniques to the description of FUS and (ii) carry out simulations with this method to understand the response of a model lipid bilayer to FUS. We show that the spatial pressure gradients between the focused and free regions and between the parallel and perpendicular directions to the membrane are the origin of the mechanism. This induces opposite lipid flows between the focused and free regions, which then create wrinkles along the diagonal of the membrane at low intensity FUS and tear up the membrane at high FUS intensities. The torn membrane is still not reformed within a few microseconds.

II. METHODOLOGY

A. The system

We study the membrane composed of 1,2-dioleoyl-sn-glycero-3-phosphocholine (DOPC) lipids immersed in water. The coarse-grained MARTINI 2.2 force field^{34,35} is employed to describe the membrane and water. In this force field, a coarse-grained water bead represents four water molecules. A DOPC lipid molecule consists of

hydrophilic (NC3 and PO4) beads, hydrophobic (C1A, D2A, C3A, C4A, C1B, D2B, C3B, and C4B) beads, and intermediate (GL1 and GL2) beads [Fig. 1(a)]. The system consists of one membrane of 4592 DOPC lipids solvated in 404 960 waters. The initial dimensions of the unit cell are $(L_x, L_y, L_z) = (40, 40, 35)$ nm [Fig. 1(b)]. Starting from this configuration, an equilibrium MD simulation is carried out for 200 ns in the NPT ensemble with the pressure $P = 1$ bar and temperature $T = 303$ K, employing the GROMACS simulation package.³⁶ The last structure is used as the initial structure for subsequent NEMD simulations.

B. Focused ultrasound simulation method

In FUS experiments, ultrasound is only applied to a given region, called focused region, of the system whose local pressure varies in time following the external sound wave pressure. The rest, called free region, is supposed to be much larger, whose pressure is maintained at the equilibrium biological pressure P_0 of the

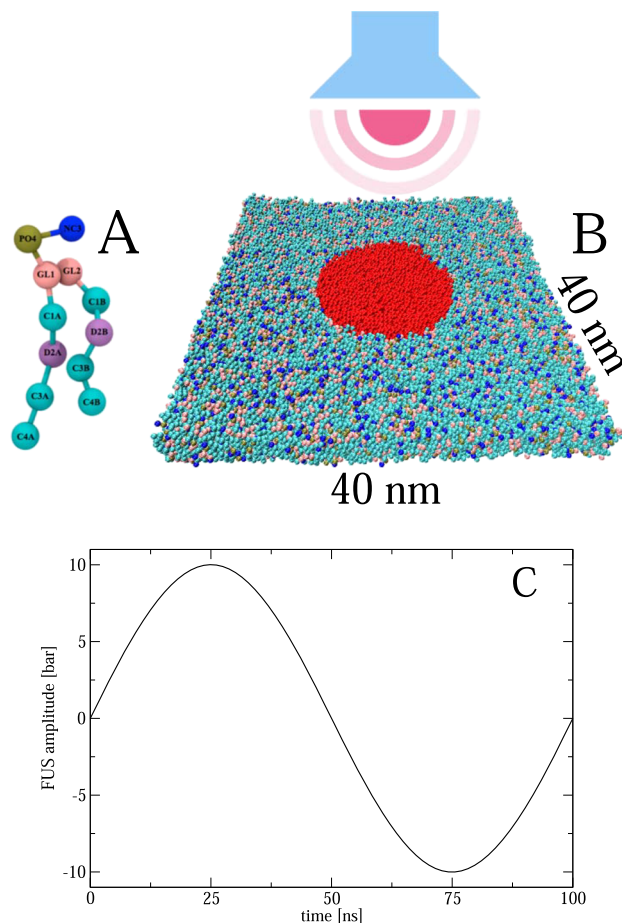


FIG. 1. (a) The MARTINI coarse-grained DOPC lipid model and (b) initial structure of the system with edge lengths $(L_x, L_y, L_z) = (40, 40, 35)$ nm. For clarity, water is not shown. The ultrasound is focused to the region colored in red, having the radius $R = 8$ nm and centered at the center of the simulation box. (c) One period of 100 ns of the ultrasound pressure.

system. To simulate this type of experiment, we suggest to couple two regions to different barostats. In the free region, the standard Berendsen barostat³⁷ is used to maintain the biological pressure P_0 . This is achieved by scaling coordinates of atoms $\mathbf{r}_i = \mu \mathbf{r}_i$ ($i = 1 \dots N_{fr}$) with the scale factor

$$\mu = \left[1 - \frac{\Delta t}{\tau_p} (P(t) - P_0) \right]^{1/3}. \quad (1)$$

Here, N_{fr} is the number of atoms belonging to the free region, Δt is the integration time step, τ_p is the coupling time to the barostat, and $P(t)$ is the instantaneous pressures. In the focused region, the effect of the sound wave, which has the form [Fig. 1(c)],

$$p(t) = A \sin\left(\frac{2\pi\tau}{t}\right), \quad (2)$$

is taken into account by scaling the coordinate of atoms in this region as $\mathbf{r}_i = \mu^* \mathbf{r}_i$ ($i = 1 \dots N_{fo}$) with

$$\mu^* = \left[1 - \frac{\Delta t}{\tau_p} \left(P^*(t) - P_0 - A \sin\left(\frac{2\pi\tau}{t}\right) \right) \right]^{1/3}, \quad (3)$$

where τ and A are the period and amplitude of the ultrasound, N_{fo} and $P^*(t)$ are the number of atoms and instantaneous pressure in this region, respectively. Because the system is only perturbed locally, the overall pressure of the system is dominated by the pressure of the free region $P(t)$. Thus, it is sufficient to use only the scale factor μ in Eq. (1) to scale the length of the system $L = \mu L$ after scaling the coordinates, and the volume becomes $V = (\mu L)^3 = [1 - \frac{\Delta t}{\tau_p} (P - P_0)] V$.

C. Parameters and simulation details

The typical ultrasound period of high and low intensity FUS experiments is $\tau = 2000 - 100$ ns (frequency $\omega = 0.5 - 10$ MHz).^{38,39} The ultrasound pressure amplitudes for high and low intensity FUS experiments are in the range $A = 10 - 100$ bars⁴⁰ and $A = 1 - 10$ bars,³⁹ respectively. To be computationally feasible with available computer resources, we use FUS with period $\tau = 100$ ns ($\omega = 10$ MHz), which is in the range of experiments, in all simulations, and our system size is on the order of nanometers ($L_x, L_y, L_z = (40, 40, 35)$ nm). The nanosecond-microsecond simulation time scales allow us to capture several FUS periods. The FUS pressure amplitude is varied from 0 to 55 bars, at which we first observe the tearing of the membrane. The focused region with a radius $R = 8$ nm [Fig. 1(b)] is large enough, $\sim 10\%$ of the system volume, such that the system receives sufficient energy to change the structure within reasonable simulation time scales. The GROMACS simulation package³⁶ coupled to our code of FUS is used for all simulations. The reference pressure, $P_0 = 1$ bar, the pressure coupling constant, $\tau_p = 1$ ps, and an isothermal compressibility of 3.4×10^{-4} bars⁻¹ are used. Because the free region is supposed to be much larger than the focused region, the global temperature of the system should be maintained at an equilibrium value. Therefore, we couple the whole system to the heat bath at 303 K, employing the Berendsen coupling method³⁷ with a temperature coupling constant of 0.1 ps. This ensures that the structural changes in the membrane are not due to heat generated by work done by ultrasound. The equations of motion are integrated using

the leapfrog algorithm with a small time step of 10 fs. The electrostatic interactions are calculated using the particle mesh Ewald method and a cutoff of 1.4 nm.⁴¹ A cutoff of 1.4 nm is used for the van der Waals interactions. The nonbonded pair lists are updated every 5 fs. The use of small time step, more frequent update of the pair lists, and a large neighboring list ensure that the temperature of the water is well-maintained.⁴²

III. RESULTS AND DISCUSSION

A. The system is at quasiequilibrium state

Figures 2(a) and 2(b) show, as examples, the time evolution of the pressure and temperature of the system for the simulation using a high ultrasound intensity, $A = 55$ bars. As seen, the pressure of the system always fluctuates around the reference value of 1 bar, although the large ultrasound pressure variation, between -55 and 55 bars, is applied to the focused region. This indicates that the focused region, whose volume is $\sim 10\%$ of the whole system, is indeed small enough to ensure only a local excitation. The temperature of the system oscillates with the ultrasound, but due to the coupling to the heat bath, its average value is well-maintained around the reference value of 303 K, with the oscillation amplitude of only ~ 1 K. This suggests that the simulation well mimics the quasiequilibrium states of experiments, which could be otherwise, unsafe for clinical applications if the temperature was elevated too high. These results also suggest that structural rearrangements in the membrane are not dominantly induced by high pressures and/or temperatures of the whole system. Finally, the total energy of the system [Fig. 2(c)] does not exhibit large deviations, reflecting that the system does not undergo any very large structural changes as seen below.

B. FUS induced structural change in the membrane

To obtain the first impression on the FUS induced rearrangements in the membrane, we show in Figs. 3(a) and 3(b) the order parameter P_2 of lipids belonging to the free and focused regions, respectively. Here, P_2 is calculated as⁴³

$$P_2 = \frac{1}{2N} \sum_{i=1}^N \frac{3}{2} \left(\mathbf{u}_i \cdot \mathbf{d} \right)^2 - \frac{1}{2}, \quad (4)$$

where \mathbf{u}_i is the unit vector, connecting the two end particles, namely, PO4 and C4A [Fig. 1(a)] of a lipid, \mathbf{d} (the director) is a unit vector defining the preferred direction of alignment of lipids, and N is the number of lipids in the focused or free region. First, it is clear that the focused region interacts directly with FUS, and thus it is more disordered than the free region. Second, the system tends to be disordered during the ultrasound compression phase and then recovers to the ordered states upon the ultrasound expansion. FUS with low intensities, $A \leq 10$ bars, does not induce much changes in the order of lipids with P_2 is always ≈ 0.5 in both regions. With a stronger ultrasound, $A = 30$ bars, the lipids in the focused region become more disordered with P_2 reduces from the initial value of 0.5 to 0.4 at 600 ns, and the free region is slightly disordered. With intensities ≥ 50 bars, the lipids in the focused region are very disordered with the lowest value $P_2 \approx 0.1$ when FUS reaches the maximum intensity. The free region also becomes disordered with the lowest value $P_2 \approx 0.3$. After six compression and expansion periods of FUS, the membrane

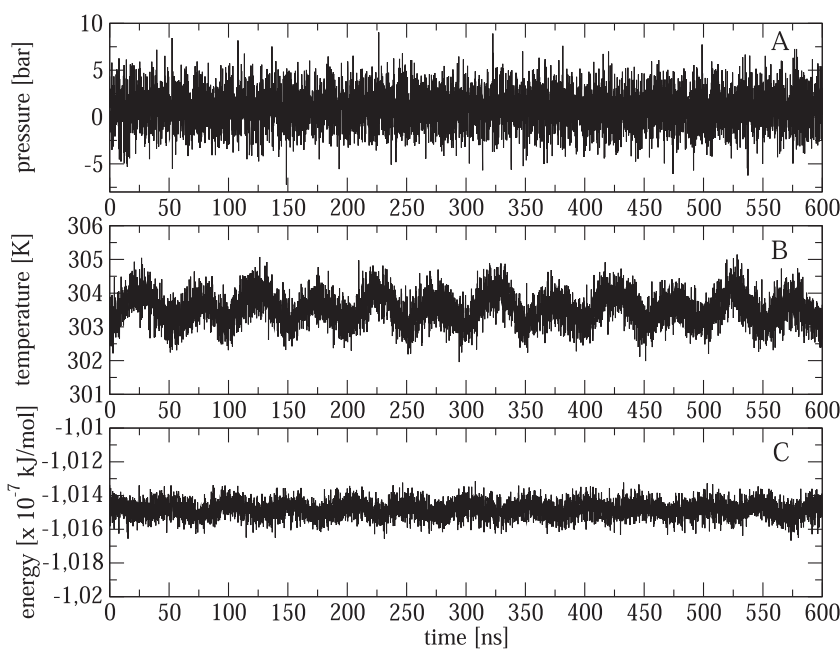


FIG. 2. Time evolution of the pressure (a), temperature (b), and total energy (c) of the system simulated by using FUS with intensity $A = 55$ bars and period $\tau = 100$ ns.

is distorted as illustrated by selected snapshots shown in Figs. 4(a) and 4(b).

Initially, the membrane is basically flat, and the lipid density is homogeneous [Fig. 1(b)]. Under FUS with amplitude $A = 30$ bars,

the membrane tends to be more and more bended as seen from the selected snapshots at 225 and 600 ns. Then, the membrane is wrinkled along the diagonal, and the lipid density is inhomogeneous (snapshot at 2800 ns) [Fig. 4(a)]. A similar picture is observed with

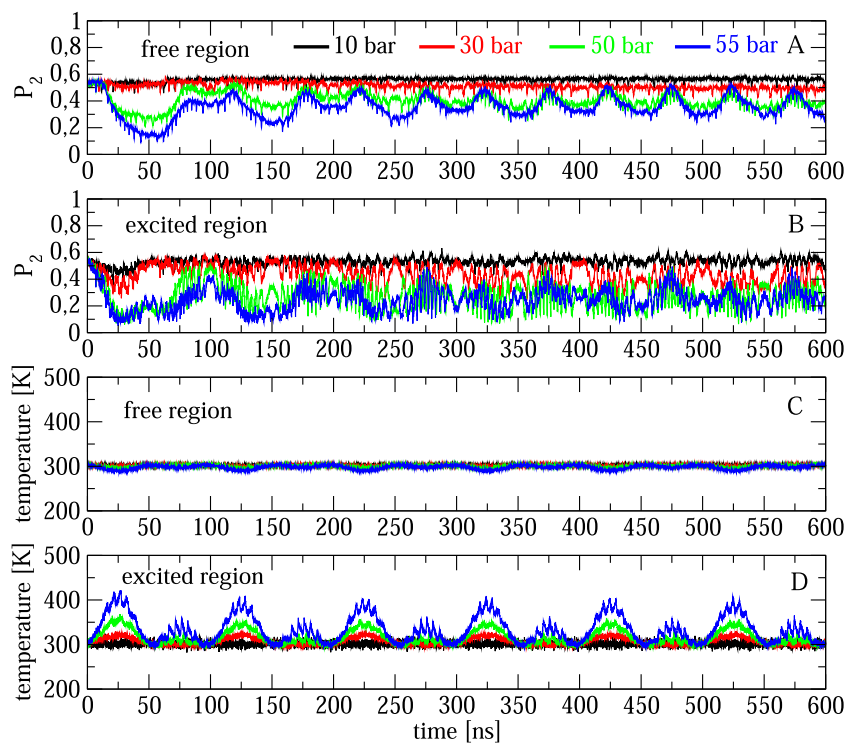


FIG. 3. Time evolution of the order parameter P_2 and the temperature of the lipids pertaining in the free region (a) and (c), and in the focused region (b) and (d). Shown are results obtained by using FUS with $\tau = 100$ ns and different amplitudes A .

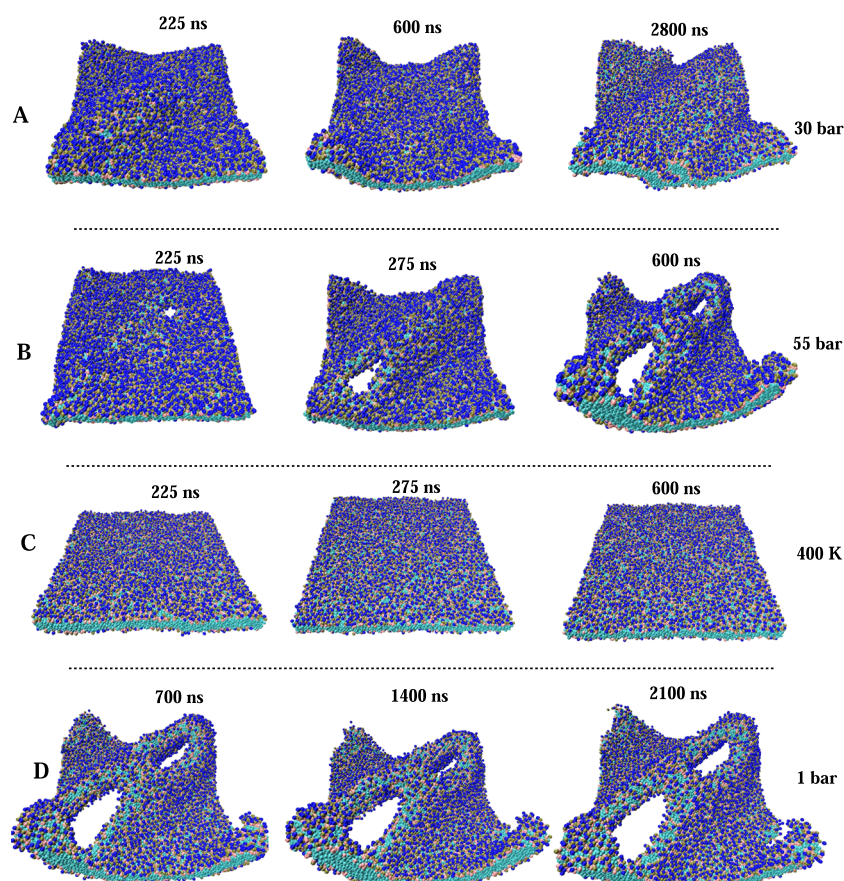


FIG. 4. The snapshots of the membrane at the selected time steps obtained from NEMD simulations using FUS intensity $A = 30$ bars (a), $A = 55$ bar (b), and from the equilibrium simulation at the temperature of 400 K (c). These simulations start from the initial structure shown in Fig. 1(b). The snapshots shown in (d) are obtained from the equilibrium simulation at 303 K and 1 bar, starting from the structure shown in (b) at 600 ns.

$A = 50$ bars (data not shown). However, increasing the intensity to $A = 55$ bars, we observe that the membrane is not only bended and wrinkled but also torn up. A small hole appears at 225 ns and then quickly becomes larger with size, ~ 7 nm, around 275 ns. Around 600 ns, another hole appears along the diagonal, and the membrane is significantly distorted and tends to be torn up [Fig. 4(b)]. In the following, we investigate in detail the molecular mechanism of the interaction between the membrane and FUS.

C. Molecular mechanism of FUS and membrane interaction

Recently, Adhikari and colleagues have studied the membrane poration induced by the shock wave and shown that the pressure distribution maps obtained at the membrane position accurately reflect the mechanism of the shock wave on the membrane.⁴⁴ Therefore, to understand how waters and lipids respond to FUS, we calculate the 2-dimensional pressure maps showing the pressure across the X and Y axes of the membrane of the equilibrium (0 ns), fully compressed (225 ns) and fully expanded (275 ns) configurations for the case of strong intensity $A = 55$ bars by using the method developed by Ollila and colleagues.⁴⁵ The results are shown in Fig. 5. We also calculate the vector field of the velocity of atoms, and results are displayed

in Fig. 6. At the molecular level, an equilibrium state of the system is maintained by a balance between short-ranged repulsions and long-ranged attractions between particles. Initially at $t = 0$ ns, the system is in equilibrium and the pressure is distributed homogeneously on the membrane surface with small fluctuations [Fig. 5(a)]. The atoms also move randomly in all directions as seen from the velocity vector fields projected on the XOZ and XOY planes [Figs. 6(a) and 6(b)]. Upon ultrasound compression, i.e., positive ultrasound pressure shown in Fig. 1(c), lipids come closer to each other; therefore, the short-ranged repulsions increase, and the pressure in this region becomes higher than that in the surrounding free region, generating a spatial pressure gradient between two regions. Waters in the focused region are also compressed and move into the interior of the system as indicated by the direction of the velocity vector field [Fig. 6(c)]. This compresses the membrane along the Z-axis, generating another spatial pressure gradient between the perpendicular and parallel directions to the membrane plane. As a consequence, the pressure in the focused region is higher than that in the free region as shown in Fig. 5(b), and this forces lipids to move out of the focused region in the XOY plane of the membrane. Because the membrane is laterally compressed along the X and Y axes, the sum of the compress forces along X and Y will be strongest along the diagonal of the square membrane. Therefore, the membrane undergoes largest structural changes along the diagonal, and lipids

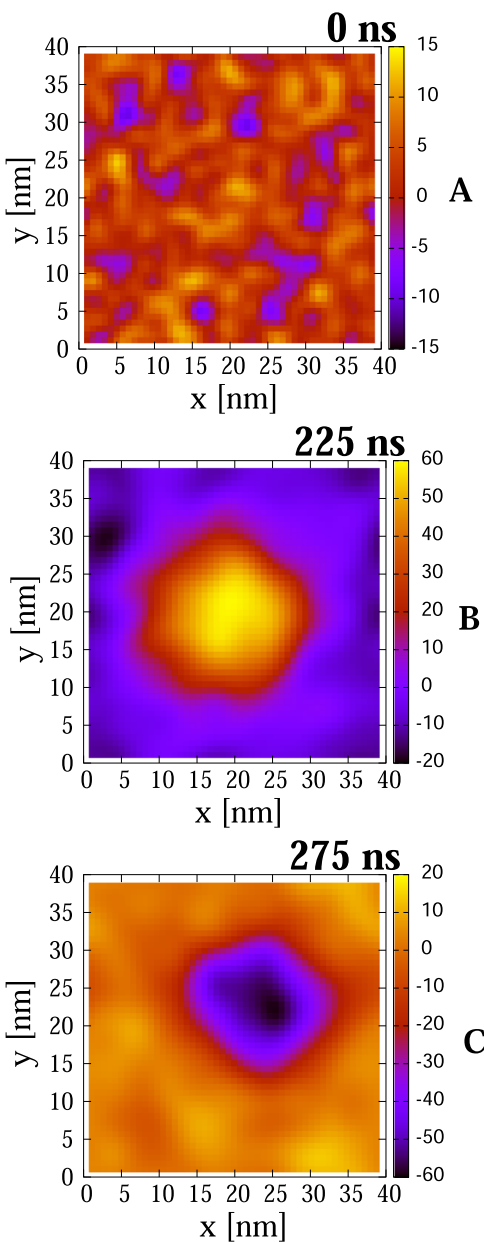


FIG. 5. The 2-dimensional pressure (in bar) maps at the membrane position at 0 ns (a), 225 ns (b), and 275 ns (c), corresponding to the initial, fully compressed, and fully expanded configurations, respectively. Shown are results obtained using FUS with $A = 55$ bars and $\tau = 100$ ns.

move preferably along this direction from right to left as shown in Fig. 6(d). Interestingly, we observe that the lipids and waters in the free region tend to move in the opposite direction, i.e., from left to right. This implies that the linear momentum is surprisingly well-conserved in the simulation system. Upon ultrasound expansion, i.e., negative ultrasound pressure, the lipids and waters are pulled apart. The attractive interactions, including the Coulombic

interaction, intramolecular lipid bending, and torsion interactions, and short-ranged van der Waals attractions become dominants, and the pressure in this region becomes negatively lower than that in the surrounding free region [Fig. 5(c)]. The waters in the focused region tend to move out of the interior of the system [Fig. 6(e)], and their direction of motion is opposite to that in the compression phase [Fig. 6(c)]. Lipids in this region also follow the motion of waters, forming a lipid flow along the membrane diagonal from left to right as shown in Fig. 6(f). Again, the lipids and waters in the free region move oppositely from right to left.

The opposite motions shown above tend to create an empty space between the tails of the lipid flow in the focused region and its counterpart in the free region, as shown in Figs. 6(d) and 6(f), and this is the origin of the mechanism that tears up the membrane. The higher the ultrasound intensity, the faster the lipid diffusion and the easier the tearing. Indeed, we calculate the lateral diffusion coefficient, $D = \lim_{t \rightarrow \infty} \frac{1}{4tN} \sum_{i=1}^N \langle [\mathbf{r}_i(t) - \mathbf{r}_i(0)]^2 \rangle$, of lipids as a function of the ultrasound intensity A . Here, the sum runs over all N lipids, and \mathbf{r}_i are the center-of-mass positions of lipids projected on the plane of the membrane. The bracket $\langle \dots \rangle$ denotes an average over different origins of time. The results are listed in Table I. Without ultrasound, i.e., $A = 0$ bar, the diffusion coefficient is $\sim 8 \times 10^{-7}$ cm 2 s $^{-1}$, which is consistent with simulations and experiments indicating the lateral diffusion coefficient to be about 10^{-7} cm 2 s $^{-1}$ in the fluid phase for single-component membranes.^{46–49} As the ultrasound intensity increases, the lipids diffuse faster with higher diffusion coefficients, and at high enough intensities, the empty space becomes bigger, and finally the membrane is torn up. Interestingly, lipids diffuse faster in the ultrasound expansion phase as compared to the compression phase. This is due to the fact that atoms have more space to move when the system is expanded.

The work done by the ultrasound generates heat, which is then removed by the heat bath so that the global temperature of the whole system is maintained at the reference value, as shown in Fig. 2(b). However, the focused region could be locally heated up upon ultrasound compression, and this could induce structural changes in the whole membrane. To understand whether this is the mechanism happened in our simulations, we calculate the temperature of the free and focused regions and results are shown in Figs. 3(c) and 3(d), respectively. Because the volume of the free region is $\sim 90\%$ of the system; thus, it is not surprised that its temperature only undergoes small fluctuations around 303 K for all ultrasound intensities. In contrast, the focused region is much smaller and interacts directly with the ultrasound; thus, it receives substantially heat. For example, the temperature of the focused region reaches maximum values of ~ 320 , 356, and 400 K when the amplitude of the ultrasound reaches the maximum values of 30, 50, and 55 bars, respectively, at $t = (2n + 1)\tau/4$ ($n = 0, 1, 2, \dots$). To check whether these high temperatures could induce changes in the membrane, we carry out an equilibrium MD simulation, i.e., without FUS, at a temperature of 400 K for 600 ns. As seen from the snapshots at three selected times shown in Fig. 4(c), the membrane is hardly affected. This suggests that structural changes in the membrane shown in Figs. 4(a) and 4(b) are not directly due to heat. Recently, NEMD simulations of the shock wave have reported the extremely high temperature with coarse-grained force fields, and this could be due to the reduction in the number of degrees of freedom.^{50–52} Thus, the high local temperature in the focused region observed in our simulations could

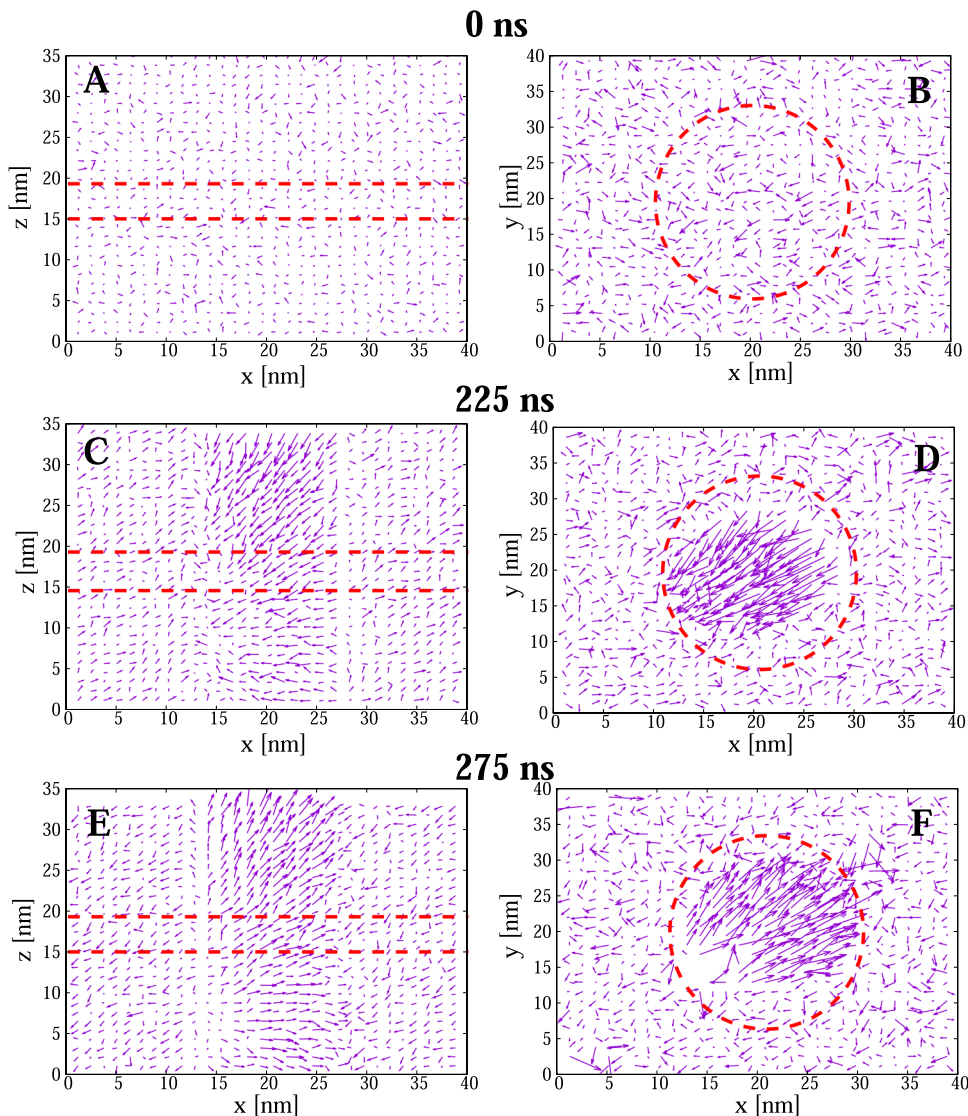


FIG. 6. The vector field of velocity of atoms projected on the XZO [(a), (c), and (e)] and XOY [(b), (d), and (f)] membrane plane at 0 ns [(a) and (b)], 225 ns [(c) and (d)], and 275 ns [(e) and (f)], corresponding to the initial, fully compressed, and expanded configurations, respectively. The directions of vectors indicate the directions of motion of atoms. Shown are results obtained using FUS with $A = 55$ bars and $\tau = 100$ ns. Inside the red circle [(b), (d), and (f)] is the focused region and between two red straight lines is the membrane [(a), (c), and (e)].

be a consequence of the use of the coarse-grained force field. This could be improved, for instance, by using the polarizable MARTINI water model.⁵² Nevertheless, because heat is not the main effect on the membrane damage in our study, thus we believe that the above-obtained mechanism of FUS induced membrane damage is still valid.

We should mention that the membrane could be damaged due to the shock wave.^{26–30,44} It has been suggested that gas bubbles could be formed within the membrane due to the nucleation.⁵³ Krasovitski and colleagues construct a mathematical model and show that bubbles are formed due to the separation of bilayer leaflets upon ultrasound expansion.⁵⁴ Okumura and Itoh carried out a NEMD simulation of an amyloid fibril system under ultrasound using a very high frequency of 1000 MHz and intensity of 3000 bars, and the ultrasound is not focused but applied to the whole system.⁵⁵ Because of very fast frequency and high intensity, the system expands in size

quickly and largely upon ultrasound expansion, leaving large empty spaces, i.e., bubbles in the system. In all cases, bubbles are collapsed during the ultrasound compression, and damage surrounding. To understand whether this is the mechanism happened in our simulations, we detect cavitation in the system by computing the number of density on 3D grids. More intuitively, we calculate the radial distribution functions between water-water, water-lipid, and lipid-lipid molecules when the system is fully expanded and fully compressed, but before the membrane is torn up, for the case $A = 55$ bars. As shown in Fig. 7, the radial distribution functions of the fully compressed and fully expanded configurations are virtually identical. This is attributed to the fact that our ultrasound is low in intensity, frequency and focused to a small region; thus, the system only undergoes small expansion within a long time scale, atoms have time to redistribute positions, and therefore large empty spaces are not formed in the system. Thus, the scenario about the bubble cavitation

TABLE I. Lateral diffusion coefficients of lipids as a function of the FUS amplitude. Shown are results obtained during the ultrasound compression (left) and expansion (right).

Amplitude (bars)	Diffusion coefficient ($\times 10^{-5} \text{ cm}^{-2} \text{ s}^{-1}$)	
	Compression	Expansion
0	0.08	0.08
5	22	22
10	87	89
20	341	390
30	754	886
40	1282	1567
50	1927	2355
55	2155	2530

induced membrane structural changes is excluded in our study. This conclusion is in agreement with recent experimental results.²⁰

To make contact to experiments, we should mention that early experimental studies found no effect of low-intensity ultrasound on the electricity properties of the cholesterol¹⁹ or phosphatidylcholine/cholesterol¹⁷ bilayers. Recent experiments of Prieto and colleagues have shown that bilayers, formed from solution of 1-palmitoyl-2-oleoyl-sn-glycero-3-phosphoethanolamine and 1-palmitoyl-2-oleoyl-sn-glycero-3-phospho-(1'-rac-glycerol), respond to the ultrasound by small changes in membrane area and capacitance.²⁰ The difference between these conclusions could be due to differences in experimental design, accuracy of the measurements, and bilayer properties. For example, Rohr and colleagues¹⁹ reported

a resolution of $\pm 3\%$ for their measurements of capacitance changes, which would have been insufficient to detect the small changes ($<1\%$) observed by Prieto and colleagues.²⁰ In this work, Prieto *et al.* used two ultrasound frequencies of 1 MHz and 43 MHz, and the diameters of the sound beams at the focal spot are comparable with the diameter of the membrane ($\sim 0.1 \text{ mm}$). Thus, these are essentially not focused ultrasound experiments because the ultrasound spreads over the membrane. The authors found that the ultrasound intensity gradients across the membrane and acoustic streaming in fluid along the direction of ultrasound propagation exert forces on the membrane. They suggested that these forces cause oscillation and displacement of the membrane. In our simulations, the ultrasound also interacts directly with the membrane, and the water in the focused region also exerts pressure on the membrane as shown above. However, the essential difference between experiment and simulation is that our forces exert on the focused region of the membrane, whereas experimental forces spread over the membrane surface. As a consequence, a spatial pressure gradient occurs inside the membrane, between the free and focused region, and this generates lipid flows in the membrane plane as shown above. In contrast, the membrane in the experiment moves along the ultrasound propagation which is perpendicular to the membrane surface. In short, the mechanisms of the interaction between the ultrasound and membrane are different between experiments of Prieto *et al.*²⁰ and our simulations.

Finally, a question is whether the use of the coarse-grained force field MARTINI affects the mechanism shown above? This force field has been successfully used in many equilibrium simulations of biomolecular systems, especially systems containing phospholipid membranes.³⁵ For many nonequilibrium situations, there is a need to perform a large number of simulations for a given system to

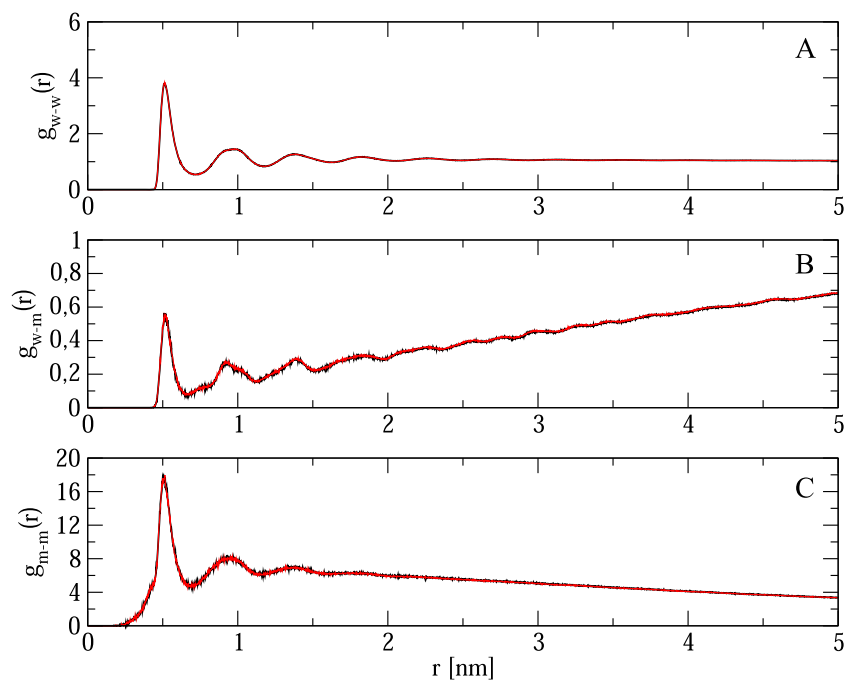


FIG. 7. The radial distribution functions between water-water (a), water-membrane (b), and membrane-membrane (c) of the fully compressed (black) and expanded (red) configurations. Shown are results obtained using FUS with $\tau = 100 \text{ ns}$ and amplitude $A = 55 \text{ bars}$.

accumulate ensemble statistics. Our system in the atomistic representation would contain nearly 2.3×10^6 atoms, and MD simulations for this system on the μs time scales would represent an enormous task. In the previous studies, the MARTINI force field has been used in NEMD simulations to study the bubble collapse induced dynamics in lipid membranes,^{22–25,27–30,32,44,52} stress propagation through lipid bilayers,⁵⁶ and pore formation by the external electric field.⁵⁷ Overall, the results are quite in good agreement with experiments or atomistic simulation results. This gives us confidence, and we believe that the essential physics of the interaction mechanism between FUS and membrane shown above is valid.

D. Reformation of the damaged membrane

It is of interest to see whether the damaged membrane is reformed under the equilibrium condition. To this end, we carry out a standard NPT equilibrium simulation without FUS, starting from the torn snapshot shown in Fig. 4(b) at 600 ns. The semi-isotropic pressure coupling is imposed along Z and X, Y directions. After $2.1 \mu\text{s}$, the membrane is still torn up with holes being not closed [Fig. 4(d)]. This suggests that the membrane is really damaged and it would take much longer time to recover the initial structure.

IV. CONCLUSIONS

We have developed a NEMD simulation method to include FUS into standard MD simulations. From the methodological point of view, this is the first molecular dynamics approach in the field, opening a new way to simulate the local interaction of ultrasound with not only membranes but also other systems. The method is applied to study the molecular interaction between FUS and a model lipid membrane DOPC. We acknowledge that our system size as well as the size of the focused region (in nanometer) is much smaller than those in experiments (in millimeter). In addition, to the best of our knowledge, there are no experimental results on the interaction mechanism between FUS and membranes at the molecular level. Therefore, at this stage, we cannot directly compare our results with any available experimental counterparts. However, in an attempt to link to experiments, we use the coarse-grained MARTINI force field, allowing us to run simulations for membranes on the micro second time scales. The long time scales allow us to simulate FUS with low frequencies up to 10 MHz as usually used in experiments. The simulation study allows us to make the following conclusions and suggestions. First, we show that although the focused region is locally heated up to ~ 400 K, this high temperature is not the primary cause for the membrane damages. Second, we show that gas bubbles are not formed in the bulk water or at the water-membrane interface or inside the membrane. Therefore, the structural change in the membrane is not due to the ultrasound induced bubble cavitation, at least in our study, as suggested by previous experiments and simulations.^{53–55} Third, we show that the origin of the molecular mechanism of FUS induced membrane damages is the spatial pressure gradients between the focused and free regions and between the parallel and perpendicular directions to the membrane. These gradients induce two opposite lipids flows between the focused and free regions. This creates wrinkles along the diagonal of the membrane at low intensity FUS. At high enough FUS intensities, these relative opposite motions are fast enough to tear up

two regions. We believe that this is a generic mechanism which plays a dominant role in the FUS induced membrane structural changes. However, the time scale of those changes should depend on (i) the ratio between the volume of the focused and free regions and (ii) the height of the water columns above and below the focused membrane region. Given a value of FUS intensity, if the focused region is too small compared to the free region, then the spatial pressure gradient between two regions could be too small. Similarly, if the water columns are too short, then the spatial pressure gradient between the perpendicular and parallel directions to the membrane surface is also too small. In both cases, the opposite lipid flows between two regions are slow and thus not strong enough to tear up the membrane. This suggests that in real applications, one has to choose suitable sizes for the focused region, depending on a given system, to minimize the damage of the membrane. Otherwise, once the membrane is torn up, it is not easy to reform. Our simulation results imply that the use of high intensity FUS could easily damage the cell membranes. The low intensity FUS does not tear up the membrane but may induce membrane wrinkling, thus changing the membrane area and capacitance.²⁰ This may stimulate endocytosis, inducing cells to uptake drugs bound to its surface. This could be another mechanism in addition to the transport of drugs through the opening at the tight junctions in the FUS induced BBB opening experiments.

ACKNOWLEDGMENTS

This work has been supported by the Department of Science and Technology at Ho Chi Minh City, Vietnam (Grant No. 10/2018/HD-KHCNTT), the CNRS, the Polish NCN Grant No. 2015/19/B/ST4/02721, and the National Institutes of Health (Grant Nos. R01-GM079383, R21-GM097617, and P30-DA035778). The content is solely the responsibility of the authors and does not necessarily represent the official views of the National Institutes of Health or other funding organizations. Computational support from the IDRIS, CINES, and TGCC centers (Project No. A0040710411), the Center for Research Computing of University of Pittsburgh, and the Extreme Science and Engineering Discovery Environment (Grant Nos. CHE090098, MCB170099, and MCB180045P) is acknowledged.

REFERENCES

1. A. Sarvazyan, O. V. Rudenko, and W. L. Nyborg, “Biomedical applications of radiation force of ultrasound: Historical roots and physical basis,” *Ultrasound Med. Biol.* **36**, 1379 (2010).
2. Z. Izadifar, P. Babyn, and D. Chapman, “Mechanical and biological effects of ultrasound: A review of present knowledge,” *Ultrasound Med. Biol.* **43**, 1085 (2017).
3. A. S. Elhelf, H. Albahar, U. Shah, A. Oto, E. Cressman, and M. Almekkawy, “High intensity focused ultrasound: The fundamentals, clinical applications and research trends,” *Diagn. Interventional Imaging* **99**, 349 (2018).
4. K. Hynynen, N. McDannold, N. Vykhodtseva, and F. A. Jolesz, “Noninvasive MR imaging-guided focal opening of the blood-brain barrier in rabbits,” *Radiology* **220**, 640 (2001).
5. N. McDannold, C. D. Arvanitis, N. Vykhodtseva, and M. S. Livingstone, “Temporary disruption of the blood-brain barrier by use of ultrasound and microbubbles: Safety and efficacy evaluation in rhesus macaques,” *Cancer Res.* **72**, 3652–3663 (2012).

- ⁶J. Wu, "Theoretical study on shear stress generated by microstreaming surrounding contrast agents attached to living cells," *Ultrasound Med. Biol.* **28**, 125–129 (2002).
- ⁷J. Wu, J. Ross, and J. Chiu, "Reparable sonoporation generated by microstreaming," *J. Acoust. Soc. Am.* **111**, 1460–1464 (2002).
- ⁸P. Marmottant and S. Hilgenfeldt, "Controlled vesicle deformation and lysis by single oscillating bubbles," *Nature* **423**, 153–156 (2003).
- ⁹J. WuShear, "Stress in cells generated by ultrasound," *Prog. Biophys. Mol. Biol.* **93**, 363 (2007).
- ¹⁰J. Wu and W. L. Nyborg, "Ultrasound, cavitation bubbles and their interaction with cells," *Adv. Drug Delivery Rev.* **60**, 1103 (2008).
- ¹¹S. Lee, T. Anderson, H. Zhang, T. J. Flotte, and A. G. Doukas, "Alteration of cell membrane by stress waves *in vitro*," *Ultrasound Med. Biol.* **22**, 1285 (1996).
- ¹²M. Lokhandwala and B. Sturtevant, "Mechanical haemolysis in shock wave lithotripsy (SWL): I. Analysis of cell deformation due to SWL flow-fields," *Phys. Med. Biol.* **46**, 413 (2001).
- ¹³V. G. Zarnitsyn and M. R. Prausnitz, "Physical parameters influencing optimization of ultrasound-mediated DNA transfection," *Ultrasound Med. Biol.* **30**, 527–538 (2004).
- ¹⁴H. Y. Lin and H. L. Thomas, "Factors affecting responsivity of unilamellar liposomes to 20 kHz ultrasound," *Langmuir* **20**, 6100–6106 (2004).
- ¹⁵R. K. Schlicher, H. Radhakrishna, T. P. Tolentino, R. P. Apkarian, V. Zarnitsyn, and M. R. Prausnitz, "Mechanism of intracellular delivery by acoustic cavitation," *Ultrasound Med. Biol.* **32**, 915–924 (2006).
- ¹⁶M. Aryal, C. D. Arvanitis, P. M. Alexander, and N. McDannold, "Ultrasound-mediated blood-brain barrier disruption for targeted drug delivery in the central nervous system," *Adv. Drug. Delivery Rev.* **72**, 94–109 (2014).
- ¹⁷P. Pohl, Y. N. Antonenko, and E. Rosenfeld, "Effect of ultrasound on the pH profiles in the unstirred layers near planar bilayer lipid membranes measured by microelectrodes," *Biochim. Biophys. Acta* **1152**, 155 (1993).
- ¹⁸P. Pohl, E. Rosenfeld, and R. Millner, "Effects of ultrasound on the steady-state transmembrane pH gradient and the permeability of acetic acid through bilayer lipid membranes," *Biochim. Biophys. Acta* **1145**, 279 (1993).
- ¹⁹K. R. Rohr and J. A. Rooney, "Effect of ultrasound on a bilayer lipid membrane," *Biophys. J.* **23**, 33 (1978).
- ²⁰M. L. Prieto, O. Oralkan, B. T. Khuri-Yakub, and M. C. Maduke, "Dynamic response of model lipid membranes to ultrasonic radiation force," *PLoS ONE* **8**, e77115 (2013).
- ²¹M. Shervani-Tabar, A. H. Aghdam, B. Khoo, V. Farhangmehr, and B. Farzaneh, "Numerical analysis of a cavitation bubble in the vicinity of an elastic membrane," *Fluid Dyn. Res.* **45**, 055503 (2013).
- ²²G. C. Ganzenmüller, S. Hiermaier, and M. O. Steinhauser, "Shock-wave induced damage in lipid bilayers: A dissipative particle dynamics simulation study," *Soft Matter* **7**, 4307–4317 (2011).
- ²³A. Choubey, M. Vedadi, K. Nomura, R. K. Kalia, A. Nakano, and P. Vashishta, "Poration of lipid bilayers by shock-induced nanobubble collapse," *Appl. Phys. Lett.* **98**, 023701 (2011).
- ²⁴D. Schanz, B. Metten, T. Kurz, and W. Lauterborn, "Molecular dynamics simulations of cavitation bubble collapse and sonoluminescence," *New J. Phys.* **14**, 113019 (2012).
- ²⁵A. S. K. Nomura, R. K. Kalia, A. Nakano, and P. Vashishta, "Nanobubble collapse on a silica surface in water: Billion-atom reactive molecular dynamics simulations," *Phys. Rev. Lett.* **111**, 184503 (2013).
- ²⁶K. Koshiyama, T. Kodama, T. Yano, and S. Fujikawa, "Structural change in lipid bilayers and water penetration induced by shock waves: Molecular dynamics simulations," *Biophys. J.* **91**, 2198–2205 (2006).
- ²⁷K. P. Santo and M. L. Berkowitz, "Shock wave induced collapse of arrays of nanobubbles located next to a lipid membrane: Coarse grained computer simulations," *J. Phys. Chem. B* **119**, 8879–8889 (2014).
- ²⁸K. P. Santo and M. L. Berkowitz, "Shock wave interaction with a phospholipid membrane: Coarse-grained computer simulations," *J. Chem. Phys.* **140**, 054906 (2014).
- ²⁹H. Fu, J. Comer, W. Cai, and C. Chipot, "Sonoporation at small and large length scales: Effect of cavitation bubble collapse on membranes," *J. Phys. Chem. Lett.* **6**, 413–418 (2015).
- ³⁰K. Koshiyama and S. Wada, "Collapse of a lipid-coated nanobubble and subsequent liposome formation," *Sci. Rep.* **6**, 28164 (2016).
- ³¹M. H. Viet, P. Derreumaux, and P. H. Nguyen, "Nonequilibrium all-atom molecular dynamics simulation of the ultrasound induced bubble cavitation and application to dissociate amyloid fibril," *J. Chem. Phys.* **145**, 174113 (2016).
- ³²M. H. Viet, M. T. Phan, M. Li, P. Derreumaux, W. Junmei, N. T. Van-Oanh, P. Derreumaux, and P. H. Nguyen, "Molecular mechanism of the cell membrane pore formation induced by bubble stable cavitation," *J. Phys. Chem. B* **123**, 71 (2019).
- ³³M. H. Viet, M. Li, P. Derreumaux, and P. H. Nguyen, "Rayleigh-Plesset equation of the bubble stable cavitation in water: A nonequilibrium all-atom molecular dynamics simulation study," *J. Chem. Phys.* **148**, 094505 (2018).
- ³⁴S. J. Marrink, J. Risselada, S. Yefimov, D. P. Tieleman, and A. H. de Vries, "The MARTINI force field: Coarse grained model for biomolecular simulations," *J. Phys. Chem. B* **111**, 7812–7824 (2007).
- ³⁵S. J. Marrink and D. P. Tieleman, "Perspective on the MARTINI," *Chem. Soc. Rev.* **42**, 6801–6822 (2013).
- ³⁶E. Lindahl, B. Hess, and D. van der Spoel, "GROMACS 3.0: A package for molecular simulation and trajectory analysis," *J. Mol. Mod.* **7**, 306–317 (2001).
- ³⁷H. J. C. Berendsen, J. P. M. Postma, W. F. van Gunsteren, A. Dinola, and J. R. Haak, "Molecular-dynamics with coupling to an external bath," *J. Chem. Phys.* **81**, 3684–3690 (1984).
- ³⁸S. A. Quadri, M. Waqas, I. Khan, M. A. Khan, S. S. Suriya, M. Farooqui, and B. Fiani, "High-intensity focused ultrasound: Past, present, and future in neurosurgery," *Neurosurg. Focus* **44**, E16 (2018).
- ³⁹J. J. Choi, S. A. Small, and E. E. Konofagou, "Optimization of blood-brain barrier opening in mice using focused ultrasound," in *IEEE Ultrasonics Symposium (IEEE, 2006)*, pp. 540–543.
- ⁴⁰G. T. Haar, "Safety first: Progress in calibrating high-intensity focused ultrasound treatments," *Imaging Med.* **5**, 567 (2013).
- ⁴¹T. Darden, D. York, and L. Pedersen, "Particle mesh Ewald: An $N \cdot \log(N)$ method for Ewald sums in large systems," *J. Chem. Phys.* **98**, 10089–10092 (1993).
- ⁴²S. J. Marrink, X. Periole, D. P. Tieleman, and A. H. de Vries, "Comment on: 'On using a too large integration time step in molecular dynamics simulations of coarse-grained molecular models' by M. Winger, D. Trzesniak, R. Baron, and W. F. van Gunsteren, *Phys. Chem. Chem. Phys.*, 2009, 11, 1934," *Phys. Chem. Chem. Phys.* **12**, 2254 (2009).
- ⁴³P. Nguyen, M. S. Li, J. E. Staub, and D. Thirumalai, "Monomer adds to pre-formed structured oligomers of $\text{A}\beta$ -peptides by a two-stage dock-lock mechanism," *Proc. Natl. Acad. Sci. U. S. A.* **104**, 111–116 (2007).
- ⁴⁴U. Adhikari, A. Goliae, and M. L. Berkowitz, "Mechanism of membrane poration by shock wave induced nanobubble collapse: A molecular study," *J. Phys. Chem. B* **119**, 6225 (2015).
- ⁴⁵O. H. Ollila, H. J. Risselada, M. Louhivuori, E. Lindahl, I. Vattulainen, and S. J. Marrink, "3D pressure field in lipid membranes and membrane-protein complexes," *Phys. Rev. Lett.* **102**, 078101 (2009).
- ⁴⁶P. F. F. Almeida, W. L. C. Vaz, and T. E. Thompson, "Lateral diffusion in the liquid phases of dimyristoylphosphatidylcholine/cholesterol lipid bilayers: A free volume analysis," *Biochemistry* **31**, 6739–6747 (1992).
- ⁴⁷J. Korlach, P. Schwille, W. W. Webb, and G. W. Feigenson, "Characterization of lipid bilayer phases by confocal microscopy and fluorescence correlation spectroscopy," *Proc. Natl. Acad. Sci. U. S. A.* **96**, 8461–8466 (1999).
- ⁴⁸A. Filippov, G. Oradd, and G. Lindblom, "Domain formation in model membranes studied by pulsed-field gradient-NMR: The role of lipid polyunsaturation," *Biophys. J.* **93**, 3182–3190 (2007).
- ⁴⁹T. Apajalahti, P. Niemela, P. N. Govindan, M. S. Miettinen, E. Salonen, S. J. Marrink, and I. Vattulainen, "Concerted diffusion of lipids in raft-like membranes," *Faraday Discuss.* **144**, 411–430 (2010).

- ⁵⁰J. K. Brennan, M. Lisal, J. D. Moore, S. Izvekov, I. V. Schweigert, and J. P. Larentzos, "Coarse-grain model simulations of nonequilibrium dynamics in heterogeneous materials," *J. Phys. Chem. Lett.* **5**, 2144 (2014).
- ⁵¹V. Agrawal, P. Peralta, Y. Li, and J. Oswald, "Pressure-transferable coarse-grained potential for modeling the shock Hugoniot of polyethylene," *J. Chem. Phys.* **145**, 104903 (2016).
- ⁵²S. H. Min and M. L. Berkowitz, "A comparative computational study of coarse-grained and all-atom water models in shock Hugoniot states," *J. Chem. Phys.* **148**, 144504 (2018).
- ⁵³A. Schroeder, J. Kost, and Y. Barenholz, "Ultrasound, liposomes, and drug delivery: Principles for using ultrasound to control the Release of drugs from liposomes," *Phys. Chem. Lipids* **162**, 1–16 (2009).
- ⁵⁴B. Krasovitski, V. Frenkel, V. Shoham, and E. Kimmel, "Intramembrane cavitation as a unifying mechanism for ultrasound-induced bioeffects," *Proc. Natl. Acad. Sci. U. S. A.* **108**, 3258 (2011).
- ⁵⁵H. Okumura and S. G. Itoh, "Amyloid fibril disruption by ultrasonic cavitation: Nonequilibrium molecular dynamics simulations," *J. Am. Chem. Soc.* **136**, 10549–10552 (2014).
- ⁵⁶C. Aponte-Santamaría, J. Brunkent, and F. Grater, "Stress propagation through biological lipid bilayers *in silico*," *J. Am. Chem. Soc.* **139**, 13588 (2017).
- ⁵⁷S. A. Kirsch and R. A. Bockmann, "Membrane pore formation in atomistic and coarse-grained simulations," *Biochim. Biophys. Acta* **1858**, 2266 (2016).